Capillary electrophoretic reactor for estimation of spontaneous dissociation rate of Trypsin Aprotinin complex

Subject Category: Electrophoresis

Capillary Electrophoretic Reactor for Estimation of Spontaneous Dissociation Rate of Trypsin–Aprotinin Complex

Yumiko Sasaki[1], Yosuke Sato[1], Toru Takahashi[2], Mitsuo Umetsu[3], and Nobuhiko Iki[1]*

[1] Graduate School of Environmental Studies, Tohoku University, 6-6-07 Aramaki-Aoba, Aoba, Sendai 980-8579, Japan

[2] Graduate School of Engineering, University of Fukui, 3-9-1 Bunkyo, Fukui 910–8507, Japan

[3] Graduate School of Engineering, Tohoku University, 6-6-11 Aramaki-Aoba, Aoba, Sendai 980-8579, Japan

*Corresponding author. iki@tohoku.ac.jp

Abstract

A capillary electrophoretic reactor was used to analyze the dissociation kinetics of an enzyme–inhibitor complex in a homogeneous solution without immobilization. The complex consisting of trypsin (Try) and aprotinin (Apr) was used as the model. Capillary electrophoresis provided a reaction field for Try–Apr complex to dissociate through the steady removal of free Try and Apr from the Try–Apr zone. By analyzing the dependence of peak height of Try–Apr on separation time, the dissociation rate k_d^H was obtained as 2.73×10^{-4} s^{-1} (298 K) at pH 2.46. The dependence of k_d^H on the proton concentration (pH = 2.09–3.12) revealed a first-order dependence of k_d^H on $[H^+]$; $k_d^H = k_d + k_1[H^+]$, where k_d is the spontaneous dissociation rate and was 5.65×10^{-5} s^{-1}, and k_1 is the second-order rate constant and was 5.07×10^{-2} M^{-1} s^{-1}. From the k_d value, the half-life of the Try–Apr complex at physiological pH was determined as 3.4 h. The presence of the proton-assisted dissociation can be explained by the protonation of $-COO^-$ of the Asp residue in Try, which breaks the salt bridge with the $-NH_3^+$ group of Lys in Apr.

Keywords: Capillary electrophoresis, Dissociation kinetics, Biomolecular complex, Trypsin, Aprotinin, Enzyme, Inhibitor

List of Abbreviations

Apr	aprotinin
Asp	aspartic acid
BAEE	*N*α-benzoyl-L-arginine ethyl ester
CE	capillary electrophoresis
CER	capillary electrophoretic reactor
CM	carboxymethylcellulose
d.i.	deionized
EDC	1-ethyl-3-(3-dimethylaminopropyl) carbodiimide
I.D.	inner diameter
KIU	kallikrein inhibitory units
Lys	lysine
NHS	*N*-hydroxysuccinimide
O.D.	outer diameter
PBS	phosphate buffered saline
RU	resonance unit
SDS	sodium dodecylsulfate
SPR	surface plasmon resonance
TPP	tetraphenylphosphonium
Try	trypsin

1. Introduction

Biomolecular complexes, such as enzyme–substrate [1], enzyme–inhibitor [2, 3], receptor–ligand [4, 5], and antibody–antigen [6], play important roles in physiological processes. To understand the function of biomolecules, it is essential to know the thermodynamic and kinetic stabilities of the complex. In a biological system, the latter often plays a vital role because the system is dynamic, and one of the components of the complex can be steadily diluted, circulated, and easily lost from the vicinity of the biomacromolecule. Therefore, the kinetic inertness is especially important to design pharmaceuticals to bind to macromolecular targets [7]. Unless the kinetic inertness is sufficiently large, the drug–target complex readily dissociates, which results in the loss of the effect of the drug. Thus, to design a drug with a long-lasting efficacy, it is essential to assess the half-life of the drug–target. Thus far, dissociation rates are estimated using techniques such as chromatographic separation, fluorescence polarization spectroscopy, recovery of biological activity, and immobilized binding partner methods [7]. Among them, the most commonly used technique is a surface plasmon resonance (SPR) device, such as Biacore^{TM}, which detects the change in refractive index induced by the binding/dissociation of the analyte to a ligand immobilized on the gold surface [8]. The SPR method has advantages such as the ability to simultaneously estimate thermodynamic and kinetic dissociation constants. However, the method has disadvantages associated with immobilization such as mass transport limitations, surface heterogeneity, possible loss of ligand activity, and dependency of the activity on the orientation of the ligand on the gold surface [9, 10]. Therefore, a method is required that enables the direct estimation of dissociation rates of biomolecular complex in a homogeneous solution without immobilization.

Recently several reviews have shed light on capillary electrophoresis (CE) owing to the high applicability to analysis and kinetic and thermodynamic characterization of protein and peptide complexes [11-14]. Prior to the works cited in those reviews, we first devised a method to analyze the spontaneous dissociation of a metal complex using CE [15], which enabled the

steady removal of the components (metal and ligand) from the metal complex zone in a homogeneous solution in the capillary. During electrophoretic separation, the complex dissociated, and the peak height of the complex exhibited a single exponential decay, $\exp(-k_d t)$, where k_d is the dissociation rate constant, and t is the separation time. By analyzing the dependence of the peak height on t, we estimated the k_d of the complex. We termed this method the CE reactor (CER) [15, 16]. Aprotinin (Apr) is a typical trypsin (Try) inhibitor existing in blood serum to bind to the active site of Try with a large association constant (10^{13} M^{-1}) and is known to prevent any Try that is prematurely activated in the pancreas from digesting that organ [17]. Because the structure and inhibition mechanism of Apr against Try have been extensively studied [18-20], here we employed the complex as an example of the enzyme–inhibitor complex to demonstrate the applicability of the CER to estimate the k_d. This approach eliminates the problems associated with component immobilization.

2. Materials and Methods

2.1. Materials

Trypsin from bovine pancreas (Activity ≥ 10,000 BAEE units/mg of protein) was obtained from Sigma Aldrich. Apr from bovine lung (50000 KIU) was purchased from Wako Pure Chemical Corp. Tetraphenylphosphonium (TPP) bromide was used as an internal standard and was purchased from Tokyo Chemical Industry Co., Ltd. All other chemicals of reagent grade were obtained from Wako Pure Chemical Corp. Deionized (d.i.) water was prepared with an Elix Advantage 5 Water Purification System (Merck Millipore) and used throughout the study.

2.2. Instruments

For the CE runs, Agilent CE 7100 equipped with a fused silica capillary (GL Sciences, I.D. = 0.05 mm, O.D. = 0.375 mm, total length, L = 100 cm, effective length, l = 91.5 cm) was used.

The pH of aqueous solutions was measured with a pH meter HM-30R (Toa-DKK) equipped with a pH electrode GST-5425. For the SPR measurement, Biacore T200 (GE Healthcare) was used with a carboxymethylcellulose (CM)-modified sensor chip (model Series S Sensor Chip CM5).

2.3. Preparation of sample solutions

To a 1.5-mL sample tube, appropriate amounts of d.i. water, phosphate buffer, 1.0 mg/mL Try solution, 0.9 mg/mL Apr solution, and TPP solution were pipetted to prepare a 200-μL sample. Finally, the tube was shaken with a vortex mixer to ensure complete mixing. Samples for the outer standard were prepared using the same approach without the addition of Apr. The final concentrations of the components are provided in the figure captions.

2.4. Determination of proton concentration

The pH values obtained with the pH meter were converted to the proton activity a_H using the following equation:

$$\mathrm{pH} = -\log a_{H.} \quad (1)$$

Furthermore, the proton concentration $[H^+]$ in M (1 M $\equiv$ 1 mol dm^{-3}) was calculated using

$$a_H = \gamma_H [H^+], \quad (2)$$

where γ_H is the activity coefficient [21] at the ionic strength of the CER buffer.

2.5. Capillary electrophoresis

The electrophoretic buffer was prepared by mixing the solutions of H_3PO_4 and NaH_2PO_4 to

adjust the pH ($[H_3PO_4]_{Total}$ = 70 mM). The capillary was washed thoroughly with 1.0 M NaOH and 1.0 M HCl for 5 min each with 1 bar. Then, it was washed with a 0.01 M sodium dodecylsulfate (SDS)–0.01 M NaOH mixture, d.i. water, 0.1 M HCl, and d.i. water for 10 min each. Then, the electrophoretic buffer was flushed through the capillary for 30 min. The sample solution was injected at a pressure of 50 mbar for 2 s and electrophoresed by applying V = 8–22 kV at 298 K. Try, Apr, the complex, and TPP were detected via absorption at 200 nm.

2.6. SPR analysis

The dissociation rate of Apr from Try was determined via SPR to verify the rate obtained with CER. Try was immobilized on the CM sensor chip via activation of the carboxylate groups with the *N*-Hydroxysuccinimide (NHS)/1-ethyl-3-(3-dimethylaminopropyl) carbodiimide (EDC) mixture followed by flushing with a phosphate buffered saline (PBS) containing Try. Then, the remaining reactive carboxylates were inactivated by flushing with an ethanolamine solution. The amount of immobilized Try was determined to be 1086.2 RU. The SPR measurement was implemented using a running buffer consisting of a phosphate buffer (70 mM, pH 3.14) containing 0.005% Tween 20 at 298 K. The Apr samples (3.91–62.5 nM) were prepared in the running buffer and injected in parallel at a flow rate of 50 μL/min. The kinetic analysis was performed by global fitting a set of 5 sensorgrams to describe a 1:1 bimolecular reaction model.

3. Results and Discussion

3.1. Separation of Try, Apr, and complex with CE

Because the CER is based on the steady removal of the components from the complex zone in a capillary via electrophoresis, it is necessary for the complex and components to have different electrophoretic mobilities. To satisfy this condition, they should be separated by CE. Following the reported conditions for the CE separation of Try, Apr, and the complex [22], we used

phosphate buffer in the acidic region (pH = 2–3). Fig. 1a shows the typical electropherograms for the mixture of Try and Apr obtained at pH 2.03. The Try and Apr peaks can be assigned based on those that appear in the Apr and Try electropherograms (Figs. 1b and 1c, respectively). Apr migrated faster than Try and exhibited higher electrophoretic mobility. This is reasonable because the electrophoretic mobility tends to depend on the charge-to-mass ratio of the solutes, and Apr is more basic (pI = 10.5) and smaller (M_r = 6.5 kDa) than Try (pI = 10.0, M_r = 23.8 kDa).[23] Because the obtained electrophoretic mobility is between those of Apr and Try, a considerably large peak appeared between Apr and Try can be assigned to the Try–Apr complex, which is in agreement with a previous report [22]. It should be noted that Apr, Try, and Try–Apr were detected before TPP. Considering the charge (+1) and mass of TPP (M_r = 339.4 Da), the number of charges in Apr and Try should be considerably larger than that in TPP. Notably, many small peaks are attributed to the impurities that accompany both Apr and Try (Figs. 1b and 1c, respectively). However, these impurities did not interfere with the CER measurement, which analyzes the time dependence of the peak height of the complex (*vide infra*).

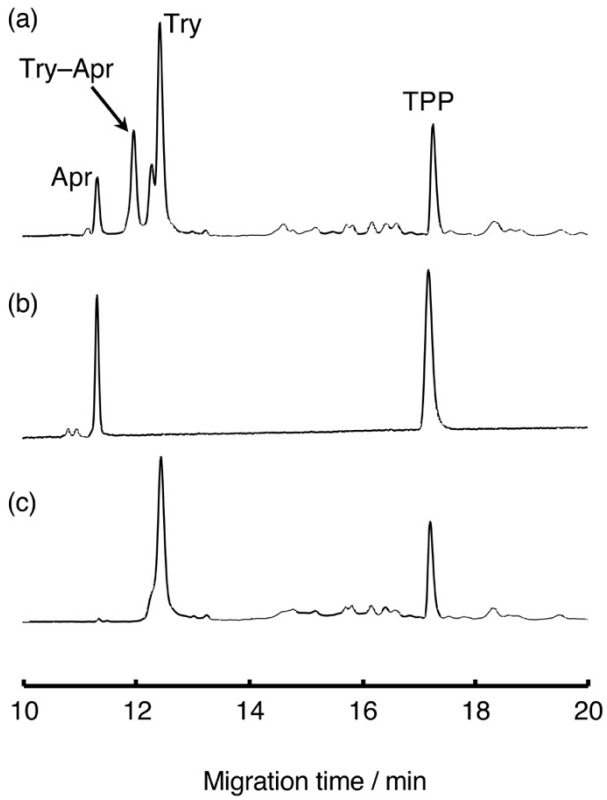

Fig. 1 Electropherograms of (a) Try–Apr mixture, (b) Try, and (c) Apr. Sample: $[Try]_{Total}$ = 4.1×10^{-5} M, $[Apr]_{Total} = 2.0 \times 10^{-5}$ M, $[TPP^+]$ = 50 μM, $[H_3PO_4]_{Total}$ = 20 mM, pH 2.03. Electrophoretic buffer: $[H_3PO_4]_{Total}$ = 20 mM, pH 2.53. V = 8 kV, I = 4.5 μA, T = 298 K.

3.2. CER analysis of Try–Apr complex dissociation

When a sample solution containing the equilibrium mixture of the Try–Apr complex and other components is placed in an electric field in the capillary, the components are steadily removed from Try–Apr by electrophoresis. This process is described by the dissociation reaction:

$$\text{Try–Apr} \longrightarrow \text{Try} + \text{Apr} \qquad (3)$$

Once they are dissociated, the components never combine to form the complex because of their steady removal. When the complex is electrophoresed for a longer time, the dissociation

reaction occurs for a longer time, which results in a reduced peak height. The electrophoresis time can be varied by changing the applied voltage. In this study, when the applied voltage was reduced from 22 to 8 kV, the migration time of the complex and the other components increased from 30 to 90 min (Fig. 2a). The peak height of the Try–Apr complex decreased as the reaction time increased, which suggests that dissociation occurred. Because peak area should contain the components Try and Apr formed by dissociation of Try–Apr, we focus on the peak top where the components do not exist. Before analyzing the dependence of the peak height on the migration time, other factors affecting the peak height should be eliminated such as the fluctuation in the injection volume of the sample into the capillary and the zone broadening caused by the diffusion of the complex during the migration in the capillary. To eliminate these factors, we used the double standardization technique that employs both internal and external standards [15]. The effect of the injection volume variation on the peak height, H, of a component can be removed by standardization with the internal standard, TPP. Thus, we obtain the peak height of Try–Apr standardized with TPP, $H'_{\text{Try–Apr}}$, using the following equation

$$H'_{\text{Try–Apr}}, = H_{\text{Try–Apr}}/H_{\text{TPP,1}} \tag{4}$$

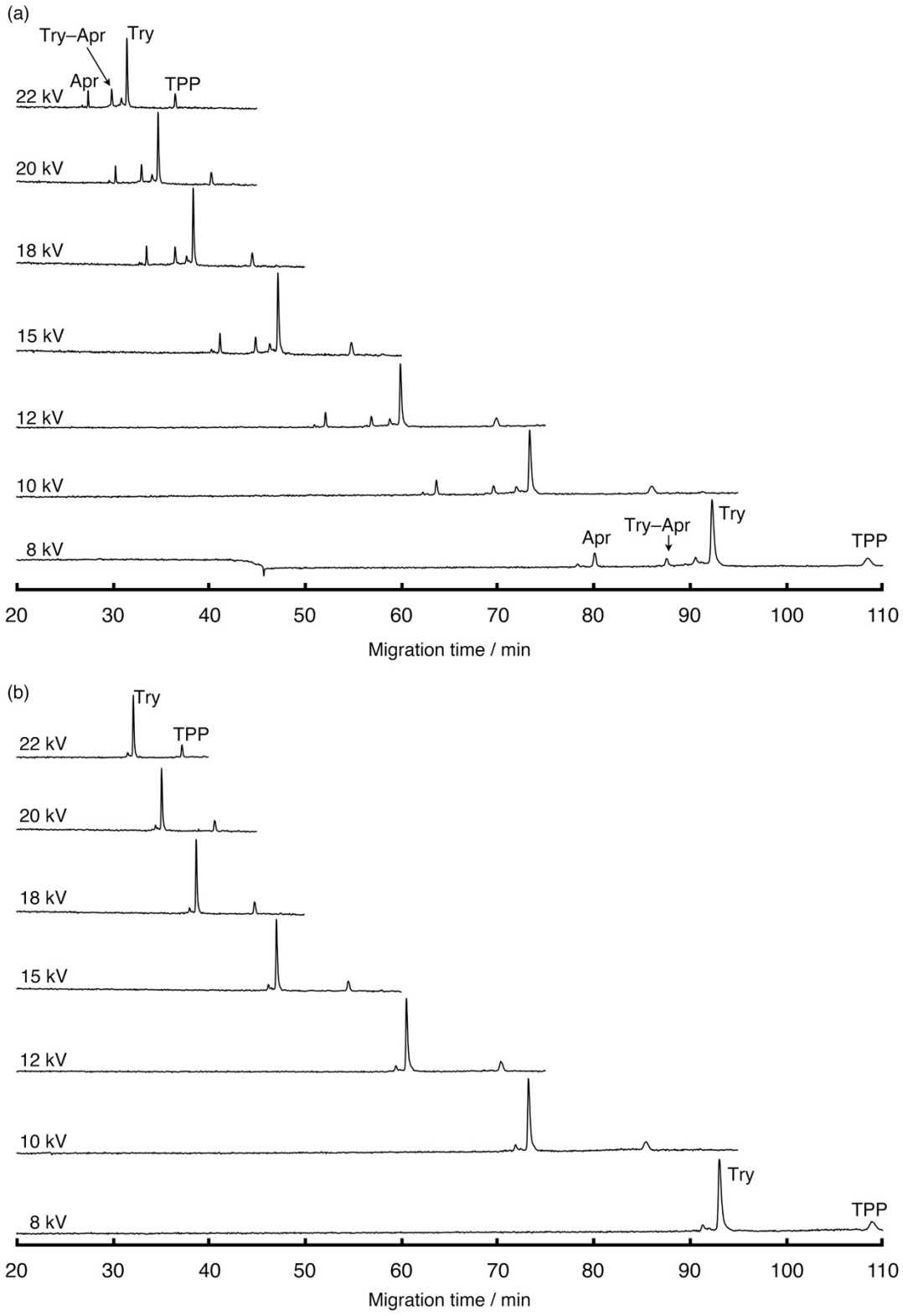

Fig. 2 Electropherograms of (a) Try–Apr complex and (b) Try as the external standard. Sample solutions: [Try] = 4.1×10^{-5} M, [Apr] = 0 or 2.0×10^{-5} M, [TPP] = 50 μM, $[H_3PO_4]_{Total}$ = 20 mM, pH 2.46. Electrophoretic buffer: $[H_3PO_4]_{Total}$ = 70 mM, pH 2.46. From top to bottom, V = 22 kV, I = 19.93 μA, V = 20 kV, I = 17.95 μA, V = 18 kV, I = 16.05 μA, V = 15 kV, I = 13.28 μA, V = 12 kV, I = 10.68 μA, V = 10 kV, I = 8.88 μA, V = 8 kV, I =7.14 μA. T = 298 K.

To remove the effect of diffusion of the complex on H', first, an external standard is required to estimate the effect. The migration time and diffusion coefficient of the external standard should be as close as possible to those of the complex. Here, we used Try as the external standard for the following reasons. First, the relative molecular masses of Try (23.8 kDa) and Try–Apr (30.3 kDa) are similar. Second, because of the proximity of the Try–Apr and Try peaks, the electrophoretic mobilities of these two components do not differ much. Therefore, Try is a suitable standard to compensate for the diffusion effect. A series of electropherograms of Try as the external standard was obtained by applying the same voltages (Fig. 2b). In addition, the variations in the injection volumes were compensated by the internal standard using the equation given below; the peak height of the external standard is standardized with TPP, H'_{Try}:

$$H'_{\mathrm{Try}} = H_{\mathrm{Try}}/H_{\mathrm{TPP,2}} \tag{5}$$

The ratio $H'_{\mathrm{Try–Apr}}/H'_{\mathrm{Try}}$ is not affected by the variance in the injection volume and dispersion of the complex zone. Therefore, it should be proportional to the concentration of Try–Apr remaining in the zone and expressed as

$$H'_{\mathrm{Try–Apr}}/H'_{\mathrm{Try}} = \alpha[\mathrm{Try–Apr}] \tag{6}$$

where α is the proportional constant. Because the spontaneous dissociation of Try–Apr is a first-order reaction, the integrated form of the reaction rate is given by

$$[\mathrm{Try–Apr}]/[\mathrm{Try–Apr}]_0 = \exp(-k_{\mathrm{d}}^{\mathrm{H}}\, t_{\mathrm{m}}) \tag{7}$$

Here, $[\mathrm{Try–Apr}]_0$, $k_{\mathrm{d}}^{\mathrm{H}}$, and t_{m} represent the initial concentration of Try–Apr at reaction time zero, dissociation rate constant at a certain proton concentration, and migration time (= reaction

time) of Try–Apr, respectively. From eqs. (6) and (7), we have

$$H'_{\text{Try–Apr}}/H'_{\text{Try}} = \beta\exp(-k_d^{\text{H}} t_m) \quad (8)$$

where $\beta = \alpha[\text{Try–Apr}]_0$. Therefore, the least squares fitting of $H'_{\text{Try–Apr}}/H'_{\text{Try}}$ against t_m from eq. (8) gives the k_d^{H} value. For example, the electropherograms obtained at pH 2.46 produced parameters such as t_m, $H'_{\text{Try–Apr}}$, and H'_{Try} (Table S1). Then, the $H'_{\text{Try–Apr}}/H'_{\text{Try}}$ values are plotted as a function of t_m (Fig. 3). By curve fitting using eq. (8), the dissociation rate constant at pH 2.46, at a temperature of 298 K was determined to be $k_d^{\text{H}} = 2.73 \times 10^{-4}$ s^{-1}. This corresponds to the half-life, $t_{1/2}$, of 42.3 min, which shows that the dissociation of this enzyme–inhibitor complex was fast at a low pH.

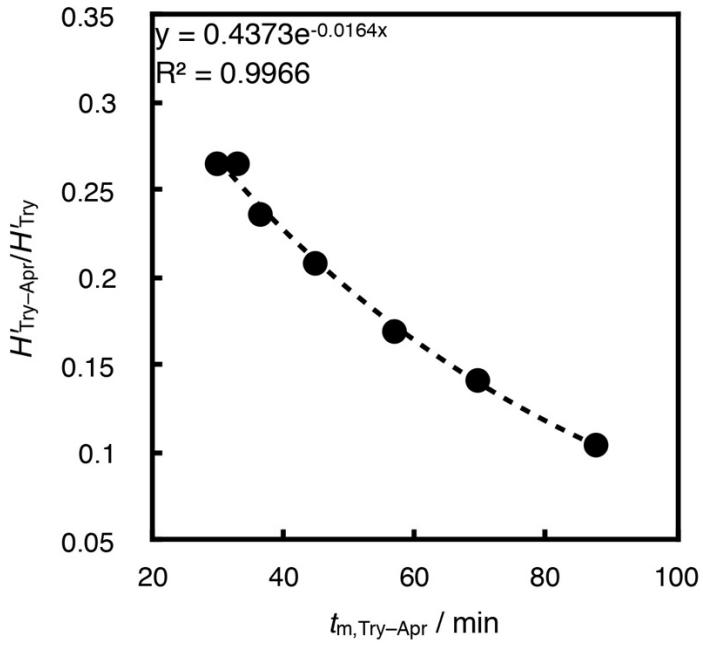

Fig. 3 Dissociation reaction profile of Try–Apr complex obtained by CER (pH 2.46, 298 K). The dashed line shows the best fit of eq. (8) with $k_d^{\text{H}} = 1.64 \times 10^{-2}$ min^{-1} (= 2.73×10^{-4} s^{-1}) and $\beta = 0.437$ ($R^2 = 0.9966$).

3.3. Proton concentration dependence of dissociation rate

To clarify whether the dissociation in the acidic pH region is promoted by protons, the dependence of the k_d^H values on the proton concentration was studied in the pH range of 2.09–3.12. For example, the electropherograms with Try as the external standard and the Try–Apr complexes at pH 2.63 are shown in Fig. S1. As can be seen, the Try–Apr peak at each voltage seems to be higher than those for pH 2.46. This observation suggests that the complex was kinetically more inert at higher pH and decelerated the dissociation. The kinetic analysis was carried out using the procedure shown in the previous section. The peak height ratios $H'_{\text{Try–Apr}}/H'_{\text{Try}}$ is plotted against $t_{\text{m,Try–Apr}}$ and fitted with eq. (8) (Fig. S2); the values are also listed in Table S2. Thus, the dissociation rate at pH 2.63 is obtained as $k_d^H = 1.37 \times 10^{-4}\ \text{s}^{-1}$ (298 K). The obtained k_d^H value is smaller than that at pH 2.46.

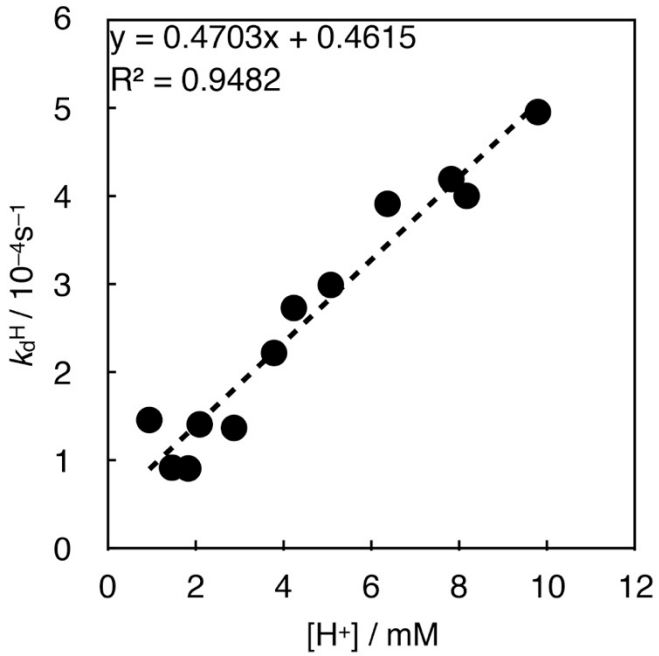

Fig. 4 Dependence of k_d^H on $[H^+]$ in the electrophoretic buffer. The dashed line shows the best fit by eq. (9) with $k_d = 4.62 \times 10^{-5}\ \text{s}^{-1}$ and $k_1 = 4.70 \times 10^{-2}\ \text{M}^{-1}\ \text{s}^{-1}$ ($R^2 = 0.9482$).

The CER measurements mentioned above were carried out at pH 2.09, 2.17, 2.19, 2.28, 2.38, 2.51, 2.77, 2.83, 2.93, and 3.12 at 298 K (Fig. S3) to obtain a set of k_d^H values (Table S3). The obtained values are plotted against the proton concentration [H^+] in the electrophoretic buffers (Fig. 4). The data fitted well with the first-order function:

$$k_d^H = k_d + k_1[H^+], \quad (9)$$

where k_d and k_1 are the intrinsic dissociation rate and proton-assisted dissociation rate constants, respectively. By the least squares fitting, the dissociation rates are obtained as $k_d = 4.62 \times 10^{-5}$ s^{-1} and $k_1 = 4.70 \times 10^{-2}$ M^{-1} s^{-1}. Because the first-order dependence of the k_d^H value on [H^+] was clear, one proton should assist the spontaneous dissociation of the Try–Apr complex. The crystallographic analysis of the Try–Apr complex clarified that the -NH_3^+ group of Lys-15 in Apr bound to the -COO^- of Asp-189, which exists in the moiety of Try, forms the salt bridge [24]. From the 541 acid dissociation constants of amino acid side chains for 78 proteins, the pK_a value of the Asp residue can be averaged as 3.5 ± 1.2 [25]. Assuming that this value is applicable to the pK_a value of Asp-189, 75–96% of the residue attaches one H^+ in the pH range of 3.12–2.09 (Table S3). This should lead to a decrease in the interaction between -NH_3^+ (Lys) and -COO^- (Asp), to result in proton-assisted dissociation. At physiological pH (= 7.40), the proton concentration is on the order of 10^{-8} M. Therefore, the proton-assisted path can be neglected (i.e., $k_d >> k_1[H^+]$), and $k_d^H \approx k_d$. Therefore, the half-life, $t_{1/2}$, of the Try–Apr complex at physiological pH can be calculated by the k_d value as 3.4 h. This value implies that the complex is kinetically inert, and the inhibition of Try by Apr should last for hours.

3.4. Validation using the SPR method

To validate the CER method, the dissociation rate was compared with the one obtained with the

SPR method. The sensorgrams were obtained with Try immobilized on the Au chip for 3.9–62.5 nM of Apr in a running buffer at pH 3.14, 298 K (Fig. S4). The simultaneous fitting of the function with two parameters ($k_d^{H,SPR}$: dissociation rate, $k_a^{H,SPR}$: association rate) to the data set provided the values of $k_d^{H,SPR} = 7.70 \times 10^{-5}$ s^{-1}, $k_a^{H,SPR} = 1.52 \times 10^5$ M^{-1} s^{-1}. We estimated the k_d^H value for the CER at pH 3.14 using eq. (10) to be $k_d^H = 8.82 \times 10^{-5}$ s^{-1} (last row in Table S3), which agrees with $k_d^{H,SPR} = 7.70 \times 10^{-5}$ s^{-1}. Thus, CER is a reliable method for estimating the dissociation rate without immobilizing a component of the biomolecular complex. In addition, the SPR method yielded the value of the dissociation equilibrium constant K_d (= $k_d^{H,SPR}/k_a^{H,SPR}$) as 5.06×10^{-10} M, which showed that the Try–Apr complex was thermodynamically stable at pH 3.14. Regardless, spontaneous dissociation cannot be ignored in the CER and SPR systems, where components are separated from each other.

4. Conclusion

This study demonstrated that CER is applicable for analyzing the spontaneous dissociation rate of the enzyme–inhibitor complex of Try and Apr. The CE using an acidic buffer can separate the Try–Apr complex and other components. Analysis of the time-dependence of the peak height of the remaining Try–Apr successfully provided the dissociation rate, k_d^H, which enabled the CER analysis. Furthermore, the dependence of k_d^H on the proton concentration successfully yielded the spontaneous dissociation rate of $k_d = 5.65 \times 10^{-5}$ s^{-1} (298 K), which showed the kinetic inertness of the Try–Apr complex with $t_{1/2} = 3.4$ h at physiological pH. In addition, using the crystallographic structure of the Try–Apr complex, the first-order dependence of k_d^H on the proton concentration can be rationalized by the protonation of the carboxylate group on Asp-189 of Try to lead to the dissociation of the Lys–Asp salt bridge, which accelerates the dissociation of Try–Apr. The validation with SPR demonstrated good agreement of the k_d^H values obtained with the CER method. Thus, CER enabled the analysis of the dissociation

kinetics of the biomolecular complex in a homogeneous solution without the immobilization of one of the components, which often lead to false results in SPR because of the mass transport limitation and heterogeneity of the surface.[9, 10]

Notes:

The authors declare no competing financial interests.

Funding Sources:

This research was supported by the Japan Society for the Promotion of Science (JSPS) through the Grants-in-Aid for Scientific Research (KAKENHI) (grant No. 17K05897).

References

[1] L.E. Tetone, L.J. Friedman, M.L. Osborne, H. Ravi, S. Kyzer, S.K. Stumper, R.A. Mooney, R. Landick, J. Gelles, Dynamics of GreB-RNA polymerase interaction allow a proofreading accessory protein to patrol for transcription complexes needing rescue, Proc. Natl. Acad. Sci. U. S. A., 114 (2017) E1081-E1090.
[2] A. Kinoshita, H. Urata, F.M. Bumpus, A. Husain, Measurement of angiotensin I converting enzyme inhibition in the heart, Circ. Res., 73 (1993) 51-60.
[3] J.S. Albert, M.W. Wood, Progress in the exploration and development of GlyT1 inhibitors for schizophrenia, John Wiley & Sons, Inc., 2012, pp. 233-254.
[4] S.C.R. Lummis, A.J. Thompson, Agonists and antagonists induce different palonosetron dissociation rates in 5-HT3A and 5-HT3AB receptors, Neuropharmacology, 73 (2013) 241-246.
[5] J. Gatfield, C.M. Grandjean, T. Sasse, M. Clozel, O. Nayler, Slow receptor dissociation kinetics differentiate macitentan from other endothelin receptor antagonists in pulmonary arterial smooth muscle cells, PLoS One, 7 (2012) e47662.
[6] C.G. Sanny, Antibody-antigen binding study using size-exclusion liquid chromatography, J. Chromatogr. B: Anal. Technol. Biomed. Life Sci., 768 (2002) 75-80.
[7] R.A. Copeland, D.L. Pompliano, T.D. Meek, Drug–target residence time and its implications for lead optimization, Nature Reviews Drug Discovery, 5 (2006) 730-739.
[8] M.A. Cooper, Optical biosensors in drug discovery, Nature Reviews Drug Discovery, 1

(2002) 515-528.
[9] E. Duverger, N. Frison, A.-C. Roche, M. Monsigny, Carbohydrate-lectin interactions assessed by surface plasmon resonance, Biochimie, 85 (2003) 167-179.
[10] P. Schuck, H. Zhao, The role of mass transport limitation and surface heterogeneity in the biophysical characterization of macromolecular binding processes by SPR biosensing, Methods Mol. Biol. (Totowa, NJ, U. S.), Humana Press Inc.2010, pp. 15-54.
[11] H.M. Albishri, S.E. Deeb, N. AlGarabli, R. AlAstal, H.A. Alhazmi, M. Nachbar, D.A. El-Hady, H. Wätzig, Recent advances in affinity capillary electrophoresis for binding studies, Bioanalysis, 6 (2014) 3369-3392.
[12] V.A. Galievsky, A.S. Stasheuski, S.N. Krylov, Capillary Electrophoresis for Quantitative Studies of Biomolecular Interactions, Analytical Chemistry, 87 (2015) 157-171.
[13] S. Štěpánová, V. Kašička, Capillary electrophoretic methods applied to the investigation of peptide complexes, Journal of Separation Science, 38 (2015) 2708-2721.
[14] A.C. Moser, S. Trenhaile, K. Frankenberg, Studies of antibody-antigen interactions by capillary electrophoresis: A review, Methods, 146 (2018) 66-75.
[15] N. Iki, H. Hoshino, T. Yotsuyanagi, A Capillary Electrophoretic Reactor with an Electroosmosis Control Method for Measurement of Dissociation Kinetics of Metal Complexes, Analytical Chemistry, 72 (2000) 4812-4820.
[16] T. Takahashi, N. Iki, Capillary electrophoretic reactor and microchip capillary electrophoretic reactor: Dissociation kinetic analysis method for "complexes" using capillary electrophoretic separation process, John Wiley & Sons, Inc.2013, pp. 127-143.
[17] D. Voet, J.G. Voet, C.W. Pratt, Fundamentals of Biochemistry: Life at the Molecular Level, 4th Edition: Life at the Molecular Level, Wiley2011.
[18] D. Krowarsch, M. Zakrzewska, A.O. Smalas, J. Otlewski, Structure-function relationships in serine protease-bovine pancreatic trypsin inhibitor interaction, Protein Pept. Lett., 12 (2005) 403-407.
[19] H.R. Wenzel, H. Tschesche, Protease inhibitors, in: C.J.A. Wallace (Ed.) Protein Engineering by Semisynthesis, CRC Press, Boca Raton, Fla, 2000, pp. 209-231.
[20] A. Paolo, B. Alessio, B. Martino, S. Andrea, C. Massimo, C. Raimondo De, M. Enea, The Bovine Basic Pancreatic Trypsin Inhibitor (Kunitz Inhibitor): A Milestone Protein, Current Protein & Peptide Science, 4 (2003) 231-251.
[21] J. Kielland, Individual Activity Coefficients of Ions in Aqueous Solutions, Journal of the American Chemical Society, 59 (1937) 1675-1678.
[22] F. Braca, F. Secco, M. Spinetti, G. Raspi, Determination of trypsin, chymotrypsin and kallikrein in porcine pancreas extracts by capillary zone electrophoresis, Chromatographia, 55 (2002) 693-699.
[23] J. Travis, I.E. Liener, The Crystallization and Partial Characterization of Porcine Trypsin, Journal of Biological Chemistry, 240 (1965) 1962-1966.
[24] K. Kawamura, T. Yamada, K. Kurihara, T. Tamada, R. Kuroki, I. Tanaka, H. Takahashi, N.

Niimura, X-ray and neutron protein crystallographic analysis of the trypsin-BPTI complex, Acta Crystallographica Section D, 67 (2011) 140-148.
[25] C.N. Pace, G.R. Grimsley, J.M. Scholtz, Protein Ionizable Groups: pK Values and Their Contribution to Protein Stability and Solubility, Journal of Biological Chemistry, 284 (2009) 13285-13289.